Mechanical Behavior of Grouted Sleeves Connections With Grouted Defects

Jiandong Bi[1,2*] and Shichao Jiang[1,2]

[1]CSCEC Road and Bridge Group CO.,LTD, Shijiazhuang, 050001, China
[2]Hebei Province Highway Engineering Green Construction Technology Innovation Center, Shijiazhuang, 050001, China

*Corresponding author. Email: jiandongbi@126.com

Abstract. Grouted sleeve splices are widely used in precast concrete buildings and bridges, due to the advantages of standardized designs, factory production, and assembly construction. To ensure the integrity of the prefabricated concrete components, the mechanical behavior of grouted sleeve connections needs to be investigated. Thus, in this study, uniaxial tensile loading and cyclic loading tests were conducted for six groups of specimens considering the influence of defective grout on the mechanical performance of sleeve connections. It is revealed that the existence of grouting defect both in the middle and end of the embedded rebar would reduce the mechanical properties (including peak strength, deformation capacity and energy dissipation capacity) of the sleeve connections. The influence of grouting defect in different locations on the strain damage of sleeve was different. The findings pointed out the detrimental impact of grouting defects on the force transmission properties of sleeve connections, the regrouting operation for the precast concrete structures is needed.

Keywords: Sleeve connections, grouting defect, peak strength, deformation capacity, strain damage.

1 Introduction

The application of prefabricated concrete structures has become more and more extensive in recent years. To maintain the structural integrity of the prefabricated structures, grouted sleeve connections were widely utilized to assemble the structural elements [1]. Therefore, the mechanical performance of grouted sleeve connections was investigated. Wu et al. [2] and Zhao et al. [3] carried out finite element analysis on the tensile performance of the grouted sleeve splices, it was found that the reduction of thickness of sleeves would lead to the reduction of tensile strength. Considering the confinement effect and rebar eccentricity, Yang et al. [4] proposed the bonding strength between rebar and grouting material. Based on tensile test, Yuan et al. [5] investigated the mechanical behavior of grouted sleeve connections under corrosion. It was found that corrosion damage of sleeves led to the strength and deformation capacity deterioration of connectors. Considering the grouting leakage, blockages and air bubbles, Xuet al. [6]

W. Nie et al. (eds.), *Proceedings of the 2024 6th International Conference on Hydraulic, Civil and Construction Engineering (HCCE 2024)*, Atlantis Highlights in Engineering 37,
https://doi.org/10.2991/978-94-6463-726-7_23

experimentally investigated the influence of grouting defects on the tensile performance of half-grouted sleeve connections. Liu et al. [7] conducted cyclic test to investigate the post-fire bond behavior of half-grouted sleeve connections with defective grouting material. Although the mechanical performance of half-grouted sleeve connections with grouting defect has been investigated, the related conclusions cannot be directly applied in fully-grouted sleeve connections which have different force transfer mechanism from half-grouted sleeve connections. Considering the broad application of fully-grouted sleeve connections in pier columns and the presence of grouting defects, this study focuses on the influence of grouting defect on the mechanical behavior of fully-grouted sleeve connections. Six groups of sleeve connections with two different types of grout defects were designed. The specimens were then tested under uniaxial and cyclic loadings. Based on the test results, load deformation curves and strain time-history curves were established. The load bearing capacity, deformation capacity, stiffness and strain distribution of the sleeve connections were analyzed. The results of this paper can provide valuable data for the service safety assessment of the assembled buildings and bridges.

2 Experimental Program

2.1 Specimen Design and Properties

In this study, six groups of grouted sleeves specimens were designed. Each group had three specimens. A photo of the representative grouted sleeve is shown in Fig. 1. The grouted sleeve was composed of sleeve, rebars and grouted material. The dimension of the sleeve is presented in Fig. 2. The total length of sleeve L was 407 mm, the distance between inlet and outlet L1 was 352 mm. The outer diameter D and minimum inner diameter D_1 and were 47 mm and 35 mm, respectively. To investigate the influence of loading patterns on mechanical performance of sleeve connections, uniaxial loading and cyclic loading were adopted. Considering that grouting defects may occur in different locations along the sleeve and therefore influence the mechanical behavior of the connections in different degree, therefore, two grouted defects were designed for the specimens as shown in Fig. 3. For grouting defect type A, the end of the embedded rebars were wrapped with double-sided tape. For grouting defect type B, the middle of the embedded rebars were wrapped with double-sided tape.

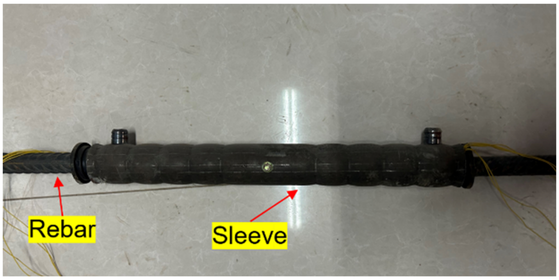

Fig. 1. Photo of the grouted sleeve connection

The high-strength grouting material was adopted in this test. The fluidity of the material was measured to be 340 mm. From the uniaxial compression tests of the prism, the compressive strength of the grouting material at 28 days was measured to be 90.5 MPa. The ultimate tensile strength of the reinforcement was 288 MPa.

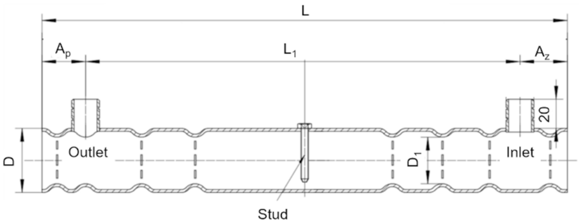

Fig. 2. Schematic dimension of sleeve

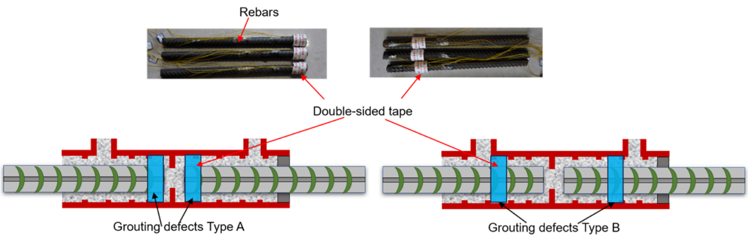

Fig. 3. Schematic diagram of sleeve defects

2.2 Loading Plan

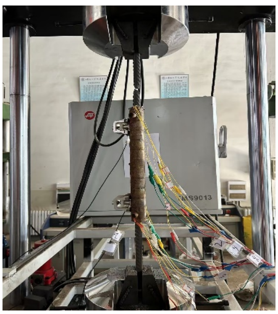

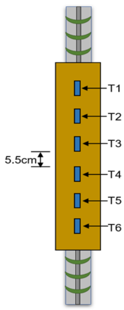

Fig. 4. Experimental equipment **Fig. 5.** Strain gauge arrangement

As shown in Fig. 4, the electro-hydraulic servo material testing machine was adopted in the test. The rebar at both ends of the sleeve was clamped by the upper and lower clamps of the machine. Then, the sleeve specimens were tested under unidirectional stretching or repeated loading. The adoption of the repeated loading is to model the condition that the prefabricated structures suffered from seismic attack. During the tests, six strain gauges (T1-T6) were symmetrically affixed along the surface of the sleeve during loading, as shown in Fig. 5. The clear distance between two adjacent strain gauges was 5.5 cm. During the loading process, the tensile force and displacement of the grouted sleeves were directly recorded. The strain was monitored by an automatic data acquisition system. The sampling frequency was set to be 1 Hz.

3 Test Results

3.1 Load Deformation Curves

Representative Specimens U1, U2, U3, R1, R2, and R3 are selected in the following analysis. The force–displacement curves are shown in Figs. 6 and 7. From Fig. 6, it can be found that each specimen experienced four stages of deformation including elastic stage, yielding stage, strengthening stage, and failure stage. Specimen U1 remained elastic before the displacement of around 3.6 mm. The corresponding value for both Specimens U2 and U3 was about 3.2 mm. From the force-displacement curve, the yielding strength of Specimen U1 was determined to be 179.3 kN. The corresponding value for Specimen U2 decreased to 168.9 kN. The reduction percentage of Specimen U3 was similar to Specimen U2. This attributed to the existence of grouting defects. From Fig. 6, it can also be found that grouting defects led to the reduction of load bearing capacity and deformation capability. Compared with Specimen U1, the peak strength of Specimens U2 and U3 were decreased from 255.7 kN to 221.7 and 234.9 kN, respectively. As for the ultimate displacement, Specimens U2 and U3 had reductions of 54.1% and 34.2% compared with Specimen U1. By calculating the enclosed area of force-displacement curves, the cumulative energy dissipation capacity of all three specimens can be determined. It can be seen that the dissipated energy of Specimens U1, U2, and U3 at failure stage were 12.64 kN.m, 4.78 kN.m, and 7.44 kN.m, respectively.

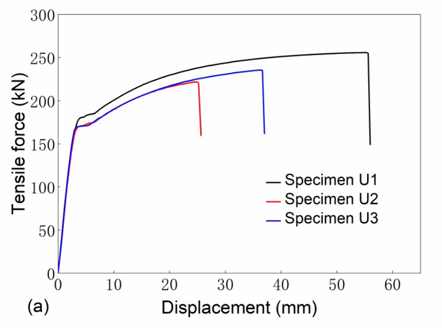

Fig. 6. Force-displacement under uniaxial loading

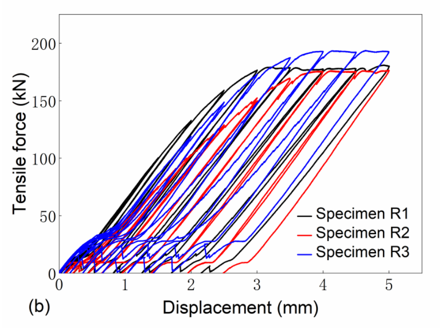

Fig. 7. Force-displacement under cyclic loading

From Fig. 7, it can be found that the specimens remained to be elastic for the first two cycles. With the further increase of repeated loading displacement, the plastic deformation was occurred which was characterized by the residual displacement. According to the force-displacement curve, the peak strength of Specimens R1, R2, and R3 were obtained to be 180.4, 176.1 and 193.3 kN, respectively. Fig. 7 also depicts that grouting defects led to the reduction of stiffness. For example, the secant stiffness at 2.5 mm of Specimen R1 was calculated to be 63.6 kN/mm. The corresponding value dropped to 59.5 kN/mm and 51.6 kN/mm, respectively.

3.2 Strain Time-History Curves

To investigate the influence of grouting defects on the mechanical properties of the sleeves, the strain time-history curves for three specimens under tensile loading are presented in Fig. 8. Fig. 8 shows that the three specimens had similar trend of accumulated tensile strain. For specimen without grouting defects, as shown in Fig. 8(a), it can be found that the value of strain gauge T3 grows from zero to 2312 με. While the corresponding value for strain gauge T1 was 2144 με. From Figs. 8(b) and (c), it can be seen that the maximum strain was 3607 and 1114 με for the specimens with grouting type A and type B, respectively. From Fig. 8, it can also be concluded that the strain damage increases from the end of the sleeve to the middle of the sleeve for each specimen. For example, at time of 2200s for specimen without grouting defect, the value of strain gauges T1, T2, T3, T4, T5, and T6 were 496, 889, 1759, 1529, 837 and 468 με, respectively. This phenomenon can be attributed to the reason that the middle part of the sleeve was the weak link of the connector. Although the trend of strain time-history curves for the three specimens was similar, the influence of the different grouting defect on the strain behavior of the sleeve was different.

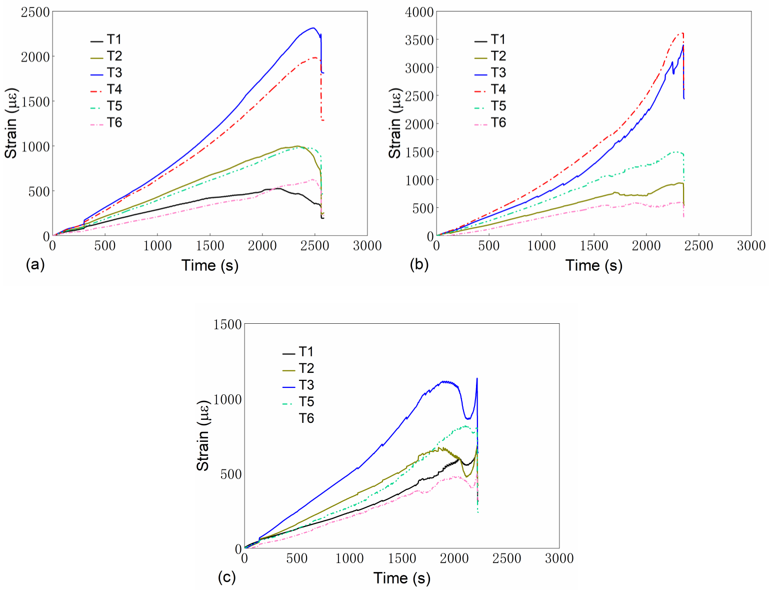

Fig. 8. Strain time-history curves: (a) Specimen U1; (b) Specimen U2; (c) Specimen U3

4 Conclusions

In this study, the influence of grout defects on the mechanical performance of sleeve connections was explored. Six groups of specimens were designed and tested under uniaxial and cyclic loading. The primary results are summarized as follows:

(1) Grouting defects led to the reduction of mechanical performance of sleeve connections, including the strength, ductility, energy dissipation capacity and stiffness.

(2) The shapes of the strain time-history curves for specimens are similar that the strain in middle part of the sleeve is larger than that in the end of the sleeve. The effect of grouting defects on the sleeve strain is not identical for different specimens.

(3) The test results will provide valuable data for further numerical simulation of the mechanical behavior of the sleeve connections and the precast concrete structures. Besides, the experimental results can lay the foundation for making scientific decisions on the maintenance and strengthening of prefabricated structures.

In future studies, numerical simulations will be conducted to investigate the mechanical behavior of grouted sleeve connections considering more parameters such as grouting defects, eccentricity of rebar, and rebar anchorage length.

Acknowledgements

The authors gratefully acknowledge the financial support provided by the "Research on grouting sleeve connection technology and seismic performance of prefabricated bridge substructure in strong earthquake areas".

References

1. Henin E, Morcous G. (2015) Non-proprietary bar splice sleeve for precast concrete construction. Engineering Structures, 83: 154-162. DOI10.1016/j.engstruct.2014.10.045.
2. Wu M, Liu HT, Du XL. (2020) Effect of tapered head sleeve structural parameters on grouting connection joints deformation. Journal of Materials in Civil Engineering, 32(5). DOI10.1061/(ASCE)MT.1943-5533.0003174.
3. Zhao CF, Zhang ZD, Wang JF, Wang B. (2019) Numerical and theoretical analysis on the mechanical properties of improved CP-GFRP splice sleeve. Thin-Walled Structures, 137: 487-501. DOI10.1016/j.tws.2019.01.018.
4. Yang C, Zhang LY, Zhang ZY, Cao XJ, Khan I, Deng KL, Xu TF. (2020) Effective stress-strain relationship for grouted sleeve connection: Modeling and experimental verification. Engineering Structures, 210. DOI10.1016/j.engstruct.2020.110300.
5. Yuan WT; Wang YR; Dong ZX; Fang QH. (2024) Experimental study on mechanical properties of corroded grouted sleeve splice. Construction and Building Materials, 412. DOI10.1016/j.conbuildmat.2023.134797.
6. Xu F, Wang K, Wang SG, Li WW, Liu WQ, Du DS. (2018) Experimental bond behavior of deformed rebars in half-grouted sleeve connections with insufficient grouting defect. Construction and Building Materials, 185: 264-274. DOI10.1016/j.conbuildmat.2018.07.050.
7. Liu QZ, Li JZ, Li MF, Wu XK, Li YC, Zhang L. (2023) Bond performance prediction model of defective grout in post-fire sleeve connections under cyclic loading. Construction and Building Materials, 400. DOI10.1016/j.conbuildmat.2023.132442.